Prestack 2D parsimonious Kirchhoff depth migration of elastic seismic data

Robert Sun*[1,2] and George A. McMechan[2]

[1]Department of Earth Sciences, National Chengkung University,
1 University Rd., Tainan, Taiwan 701
E-mail: rjsun@mail.ncku.edu.tw
Phone: +886-6-274-6459, Fax: +886-6-274-0285
[2]Center for Lithospheric Studies, University of Texas at Dallas,
800 W. Campbell Road, Richardson, Texas 75080-3021
E-mail: mcmec@utdallas.edu
Phone: (972) 883-2419, Fax: (972) 883-2829

This paper was prepared for presentation during the 12th International Congress of the Brazilian Geophysical Society held in Rio de Janeiro, Brazil, August 15-18, 2011.

Summary

We extend prestack parsimonious Kirchhoff depth migration (Hua and McMechan 2003) (which is a fast migration), to two-dimensional (2D), two-component (2C), reflected elastic seismic data, from a P-wave source. The P-to-P reflected (PP) waves and P-to-S converted (PS) waves in an elastic common-source gather recorded at the earth's surface are first separated into PP- and PS-wave seismograms. Source and receiver apparent slownesses (*p* values) are estimated for the peaks and troughs in both separated PP and PS waves. For each PP and PS reflection, a source ray is traced, in the P- (or the S-) velocity model, in the direction of the emitted ray angle (determined by the source *p* value), and a receiver ray is traced, in the P- or S-velocity model, back in the direction of the emergent PP (or the PS) wave ray angle (determined by the PP or PS wave receiver *p* value), respectively. The image point is adjusted from the intersection of the source and receiver rays to the point where the sum of the source and receiver times equals the observed two-way reflection traveltime. The orientation of the reflector surface is determined to satisfy Snell's law at the ray intersection point. The amplitude of a P-wave (or an S-wave) is distributed over the first Fresnel zone along the reflector surface in the P (or S) image. Stacking over all the single-source P- and S-images separately gives the stacked P- and S- images, respectively.

The quality of prestack parsimonious elastic Kirchhoff migration is not as good as that of full prestack Kirchhoff, or reverse-time, migration, but the computing time is reduced by orders of magnitude because the amount of ray tracing is significantly reduced. Thus, parsimonious elastic migration is most useful, when reducing computing time is more important than migration quality, such as in migration velocity analysis, which iterates migration many times.

Methodology

Prestack parsimonious elastic Kirchhoff migration can be divided into 3 steps: P-S wave separation, ray angle estimation, and imaging. Each is now described in turn.

P-S wave separation

The first step is to separate the PP and PS reflections in the elastic seismic data. In this paper we use the method of Sun and McMechan (2001). An elastic computational model is prepared. The prestack 2D elastic common-source gathers are reverse-time extrapolated from the receiver locations into this model using the 2D elastic wave equation. During reverse-time extrapolation, 2D divergence and curl common-source gathers are extracted along a horizontal line at a shallow reference depth. The elastic velocity model is then split into scalar P- and S-velocity models. The divergence is inserted into the P-velocity model at the reference depth and extrapolated using the scalar wave equation, and recorded at the original receiver locations at the surface as the separated PP waves. The amplitude of the curl (a scalar) is similarly extrapolated in the S-velocity model and is recorded at surface as the separated PS waves. With the PP and PS waves separated, they can be separately migrated.

Ray angle estimations

In elastic media, a P-wave from the source to the reflection point has an emitted ray angle θ_s and source *p* value

$$p_s = \sin\theta_s / \alpha_s, \qquad (1)$$

where α_s is the P-velocity at the source (Figure 1). A PP wave from the reflection point to the receiver has an emergent ray angle θ_{rP} (Figure 1) and receiver *p* value

$$p_r = \sin\theta_{rP} / \alpha_r, \qquad (2a)$$

where α_r is the P-velocity at the receiver. A PS wave from the reflection point to the receiver has an emergent ray angle θ_{rS} (Figure 1) and receiver *p* value

$$p_r = \sin\theta_{rS} / \beta_r, \qquad (2b)$$

where β_r is the S-velocity at the receiver.

Source *p*-values have the relation $p_s = dt/dx$ in common-receiver gathers (where *x* is the horizontal position and *t* is the time), and receiver *p*-values have the relation $p_r = dt/dx$ in common-source gathers. We estimate p_s in a common-receiver gather, and the corresponding emitted ray angle θ_s (equation 1). Then we estimate a receiver *p* value (p_{rP} or p_{rS}) in the corresponding common-source gather and determine the associated emergent ray angle θ_{rP} (or θ_{rS}) (equation 2a and b) for imaging a PP wave or a PS wave, respectively.

Ray tracing and imaging

P-velocity and S-velocity models are prepared for migration. Tracing a P-wave source ray, for the migration of both PP and PS waves, is performed in the P-velocity model in the direction of the emitted angle θ_s corresponding to the source *p*, and the source time t_s is calculated along the source ray. Tracing a receiver ray for a PP wave is performed in the P-velocity model in the direction of the emergent angle $\theta_r = \theta_{rP}$ determined using equation 2a. Tracing a receiver ray for a PS wave is performed in the S-velocity model in the direction of the emergent angle $\theta_r = \theta_{rS}$ determined using equation 2b. The receiver time t_r (of PP or PS waves) is calculated along the corresponding receiver ray for PP and PS migrations, respectively.

The intersection point of a source ray and a receiver ray provides the initial estimate of the reflection point location in migration of a PP wave or a PS wave. The local reflector orientation and the local normal line (to the local reflector) can be determined such that the incident angle ϕ_s and the reflection angle ϕ_r satisfy Snell's law at the intersection point. The intersection point is perturbed to the image point such that the travel time *t* of a peak (or trough) equals the sum of source time t_s and receiver time t_r:

$$t = t_s + t_r. \quad (3)$$

For a peak (or trough) of a PP or PS wave, the local reflector surface passes through the image point position and is perpendicular to the local reflector normal. The amplitude of a peak (or a trough) in a PP wave is added into the image over the first Fresnel zone along the local reflector in the P-image. The amplitude of a peak (or a trough) in a PS wave is similarly inserted into the S-image. All the single-source P-images are then added to obtain the stacked P-image, and the single-source S-images are added to obtain the stacked S-image.

Synthetic Example

Figure 2 shows P- and S-velocity distributions of an elastic dome/syncline model. The model has P-velocity ranging from 3.0 to 3.8 km/s and S-velocity ranging from 1.7 to 2.2 km/s. The model has a free-surface top boundary and absorbing left, right and bottom boundaries. Source locations have *x*-coordinates from 0.0 to 4.0 km with an increment of 0.04 km and *z*-coordinates of 0.03 km. Figure 3a and b shows a representative synthetic elastic common-source gather, after muting the direct arrivals and removing the surface waves, generated for this model for the source with *x*-coordinate of 1.6 km. P-S wave separation is performed on the elastic data; Figure 3c and d shows the corresponding (prestack) separated PP and PS wave seismograms (common-source gathers). The separated PP and PS wave seismograms for all sources are input for prestack parsimonious Kirchhoff depth migrations; the stacked P- and S-images are in Figure 4a and b, respectively. Comparing with the original model in Figure 2, both P- and S-images clearly show the reflectors in their correct positions, with very few artifacts.

For comparison, prestack scalar reverse-time depth migration is performed for the same separated PP and PS datasets; the stacked P- and S-images are presented in Figure 4c and d, respectively. Reverse-time migration gives better images (with fewer artifacts) than parsimonious migration does. However, the computation time for parsimonious migration is only about 1/36 of the time for reverse-time migration.

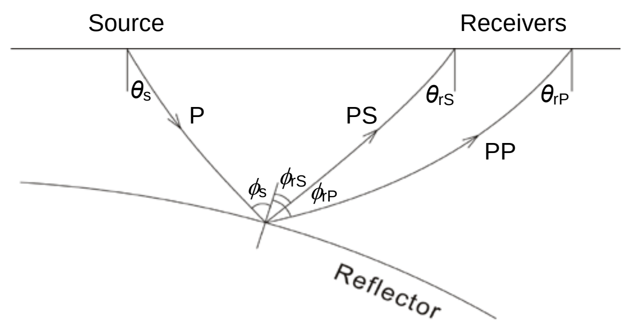

Figure 1. *Elastic wave propagation in nonhomogeneous media. P = incident P-wave; PP = P-to-P reflected wave; PS = P-to-S converted wave; ϕ_s = incident angle; ϕ_{rP} = PP wave reflection angle; ϕ_{rS} = PS wave reflection angle; θ_s = emitted angle; θ_{rP} = PP wave emergent angle; θ_{rS} = PS wave emergent angle.*

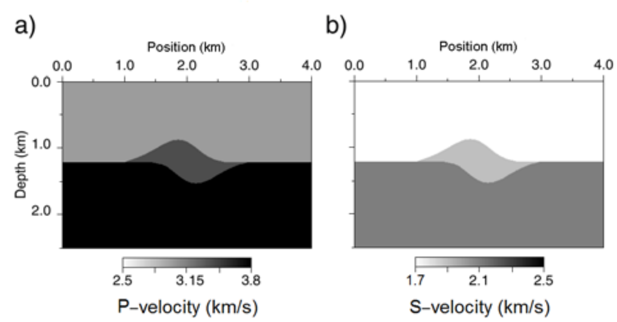

Figure 2. *A 2D elastic dome/syncline model. (a) P-velocity; (b) S-velocity.*

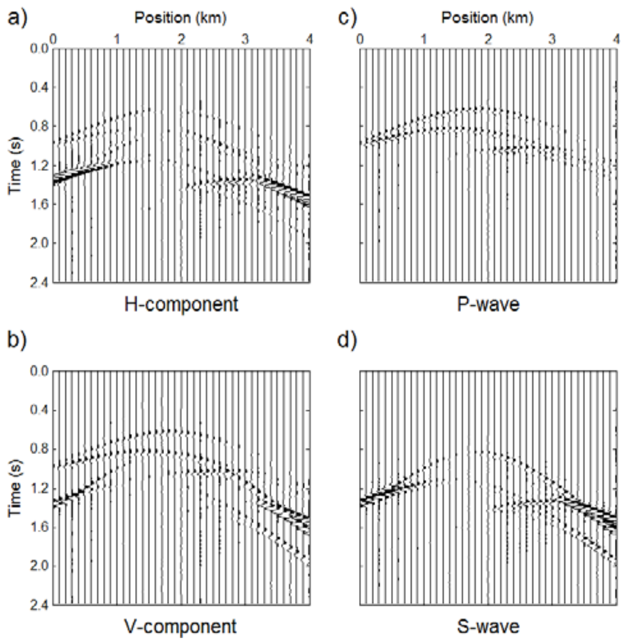

Figure 3. *Synthetic elastic common-source data generated for the elastic dome/syncline model in Figure 2. (a) and (b) are the horizontal and vertical components, respectively. (c) and (d) are the corresponding separated PP and PS common-source gathers extracted from the elastic data in (a) and (b).*

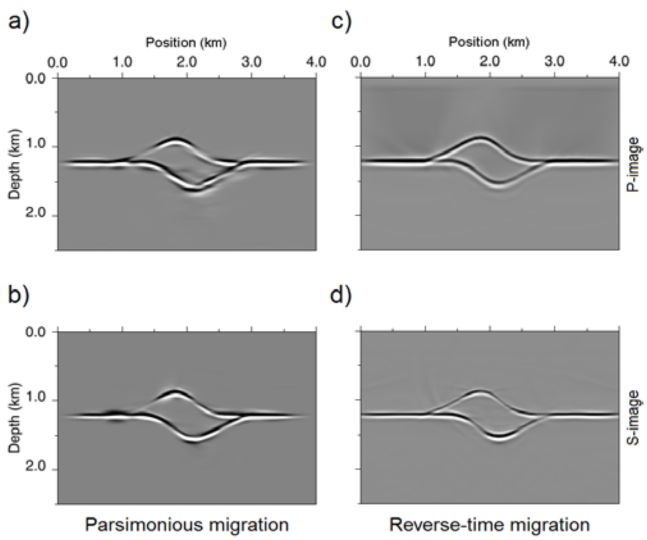

Figure 4. *Output (a) P-image and (b) S-image obtained by parsimonious elastic depth migration for the elastic data generated for the dome/syncline model in Figure 2. (c) and (d) are the corresponding images obtained by elastic reverse-time depth migration.*

Conclusions

We implement a parsimonious version of Kirchhoff prestack migration for PS reflections that is, for the examples shown, about 36 times faster than the corresponding reverse-time migration. The main steps are separation of the P and S waves, estimation of slowness and emitted/emergent angles at the source and receiver locations for each reflection to be migrated, ray tracing to estimate the reflection point, applying Snell's law to determine the reflector orientation at the reflection point, and inserting the reflection amplitude within a Fresnel zone, along the reflector, into the image, along the reflector orientation. For P-S conversion, P-velocities are used in the ray tracing from the source, and S-velocities are used in the ray tracing from the receiver.

References

Hua, B., and G. A. McMechan, 2003, Parsimonious 2D prestack Kirchhoff depth migration: Geophysics, **68**, 1043–1051.

Sun, R., and G. A. McMechan, 2001, Scalar reverse-time depth migration of prestack elastic seismic data: Geophysics, **66**, 1519-1527.